Analyst

RSC Publishing

PAPER

View Article Online
View Journal | View Issue

Cite this: *Analyst*, 2013, **138**, 1705

A mixed alkanethiol based immunosensor for surface plasmon field-enhanced fluorescence spectroscopy in serum†

Andreas Scholten,[a] Bernhard Menges,[b] Martin Juebner,[a] Markus A. Rothschild[a] and Katja Bender*[a]

Received 18th May 2012
Accepted 22nd January 2013

DOI: 10.1039/c3an35657d

www.rsc.org/analyst

This paper describes a simple and sensitive immuno-based biosensor for interference-reduced detection of C-reactive protein (CRP) in serum. The detection was performed by using a non-competitive sandwich immunoassay in combination with surface plasmon field-enhanced fluorescence spectroscopy (SPFS). CRP is an important marker for the diagnosis of inflammatory processes and cardiovascular diseases (CVD). It is nowadays detected by high-sensitivity enzyme-linked immunosorbent assays (ELISA) in blood serum. CRP was used as a model analyte in this work because it is well-characterized. However, interfering effects of matrix components affect the limit of detection (LOD) and quantification (LOQ) in general. Therefore, the availability of fast, sensitive and robust analytical methods is of major interest. A number of biosensor approaches have been described already, but only a few have demonstrated their usefulness in authentic samples such as serum. Thus our aim was to develop a simple and sensitive immunoassay-based biosensor for an interference-reduced detection of CRP in serum with surface plasmon enhanced fluorescence spectroscopy (SPFS). LODs and LOQs were experimentally determined both for CRP spiked buffer and serum. SPFS in combination with our biosensor allows sensitive analysis of CRP, achieving in buffer a LOD of 0.016 μg mL^{-1} and a LOQ of 0.049 μg mL^{-1}. In serum the accomplished LOD was 0.026 μg mL^{-1} and the LOQ was found to be 0.08 μg mL^{-1}. These low LODs and LOQs demonstrate the applicability of the designed biosensor for qualitative and semi-quantitative analysis of trace amounts of substances in very small sample volumes of body fluids.

1 Introduction

The determination of pathologically relevant marker proteins and small molecules in body fluids is very common in forensic toxicology, doping analysis and clinical chemistry. Different approaches for detecting such molecules are already well-established. Many of them are based on ELISA or related immunoassays. Due to the commonly used photometric detection of the antigen–antibody reaction the response signal can be influenced by self-absorption of light by the matrix and its composites. Furthermore, the enzymatic reaction which is relevant for the color reaction required for photometric detection can be disturbed by adulterants used for sample manipulations.[1–5] Depending on the type of the immunoassay, wrong sample pre-treatment can cause false negative results, *e.g.* addition of NaF as a common additive to inhibit metabolically active enzymes in blood samples to prevent degradation of analytes. Attempts by human test subjects to manipulate their sample are a major problem in workplace testing, doping analysis and forensic drug testing.[6,7] Attempts of adding washing detergent containing lytic enzyme to inactivate the enzyme system used in ELISAs have been reported.[8] Especially when the color reaction of the immunoassay is impeded by adulterants, novel detection methods of the actual antigen–antibody reaction or of the unlabeled antigen itself would be highly desirable, which are independent of enzymatic reactions. In principle, surface plasmon resonance spectroscopy (SPRS) and SPFS should be less prone to such disturbances, because enzymatic reactions as part of the detection are not required. The same accounts, in principle, for fluorescence-linked immunosorbent assays (FLISAs). To our knowledge, online detection by re-using the assay is not performed with FLISA based on commonly used antibody decorated microparticles. With surface bound capture antibodies, as used in our sensor design, the sensor can to some extend be re-used by regenerating the sensor surface, giving rise to the possibility for online detection. However, the literature very often emphasizes the

[a]*Institute of Legal Medicine, Medical Faculty, University of Cologne, Melatengürtel 60-62, D-50823 Cologne, Germany. E-mail: katja.bender@uk-koeln.de; Fax: +49 22147886136; Tel: +49 22147888350*

[b]*Max Planck Institute for Polymer Research, D-55128 Mainz, Germany*

† Electronic supplementary information (ESI) available. See DOI: 10.1039/c3an35657d

potency of sophisticated biosensor architectures for measurements in complex body fluids, but somehow often data of real sample measurements are lacking.

Biological matrices are very complex mixtures of small (<1 kDa, *e.g.* peptides, hormones, lipids, vitamins, drugs, sugars) and large molecules (>1 kDa, *e.g.* polypeptides, enzymes, polyglycans, DNA), and other components (*e.g.* electrolytes, gases, inorganic cations (metals) and anions), all possessing different properties. Many matrix components have a strong tendency to adsorb on surfaces.[9–12] The non-specific adsorption of matrix components on sensor surfaces can be an obstacle for the detection of the desired molecules. In the case of SPRS, the non-specific protein adsorption can overlay the detection signal caused by the specific antigen–antibody reaction.[13,14] The reason for this lies in the physical principle of SPRS which uses an evanescent wave phenomenon to detect changes in the refractive index/layer architecture on a surface.[15] The (specific or non-specific) binding of molecules induces such changes of the refractive index in the vicinity of the metallic sensor surface. To confirm the applicability of SPRS in biosensing, the detection of a wide range of molecules, but mainly in matrix-free buffer solutions, has been successfully demonstrated.[16,17] In SPRS, the detection signal only depends on the optical thickness and on the surface mass coverage, respectively. In the case of coadsorption of materials with the same refractive index, discrimination of the adsorbed materials is difficult. Interferences caused by the sample matrix increase LOD and LOQ or prevent the analyte detection completely.[18] However, in the absence of interfering matrix components very low LODs and LOQs may be reached.[18] In order to reduce interferences due to non-specific protein adsorption, several materials with antifouling properties have been developed to overcome this problem.[19–24]

Sensor assembling becomes more challenging with increasing complexity of sensor construction. This makes fabrication processes of sensors more time and material consuming and thus more expensive. Therefore, simplified sensor constructs are strongly preferable.

The label-free nature of SPRS measurements gives rise to a limitation of the ultimate sensitivity. Since SPRS effectively measures the mass density at the sensor surface, the sensitivity of SPRS is often not sufficient for direct measurements of binding events of molecules with a low molecular weight, low affinity constants or very low binding densities of larger molecules. In these cases, equilibrium analysis and competitive assays as alternatives have had to be adopted.[25–27]

By applying an indirect optical sensing approach, which makes use of the field enhancement by the evanescent wave phenomenon of SPRS, many of the limitations of direct sensing can be overcome and possibilities to increase sensitivity and selectivity are offered.[28–36] SPFS makes use of the strong evanescent field, generated by the surface plasmon, which excites fluorophores at the vicinity of the metal–dielectric interface, resulting in an amplified fluorescence signal and therefore in a good signal-to-noise ratio. Field intensity is enhanced 16-fold on gold and 50–80-fold on silver at a wavelength of $\lambda = 633$ nm.[37] Due to the stronger field intensity enhancement we utilized silver in our experiments. With the used extended SPFS set-up, both the reflected light of the surface plasmon excitation laser and the fluorescence signal can be measured simultaneously.[35,37] DNA-hybridisation and antigen–antibody reactions were successfully investigated implementing SPFS.[28,31,34,38] High sensitivities of up to atto- and femtomolar ranges are theoretically possible,[33] if no matrix interferences occur. Therefore, both methods are applied in materials science[15,39,40] and established in biosensing.[28,34,41–43]

The intention of our work is to see whether a simple biosensor in combination with SPRS or SPFS is powerful enough to fulfill the present requirement for analysis in real sample matrices. As a target analyte we chose the acute phase protein CRP and serum as the biological matrix, however in principle detection of any other analyte is possible by employing different antibodies. CRP plays an important diagnostic role in inflammatory processes and it is probably one of the best characterized marker proteins used in clinical diagnostics. Moreover, CRP provides the possibility of direct comparison of surface plasmon resonance spectroscopy (SPRS) with SPFS due to its molecular size. Due to those reasons we used CRP as the model analyte but not necessarily with the aim to replace common and well-established CRP assays. In the following paragraphs we give an overview about CRP and clinically relevant CRP concentrations as well as on sensitivities of other biosensors used for CRP detection.

In cases of infection, the CRP concentration in blood can rise up to thousand-fold of the physiological concentration.[44,45] Furthermore, CRP is also discussed as an additional indicator for estimating the risk of developing cardiovascular diseases (CVD).[46,47] According to the American Heart Association, a CRP concentration below 1 μg mL^{-1} indicates a very low risk, between 1 and 3 μg mL^{-1} a normal risk and above 3 μg mL^{-1} a higher risk for the development of CVD.[48]

Due to its diagnostic importance, many commercially available CRP determination methods in blood, mainly based on ELISA or turbidimetric immunoassays, are well-established.[49–53] The LOD of commercialized turbidimetric assay ranges from 0.03–0.3 μg mL^{-1} and LOQ from ~0.1 to 0.6 μg mL^{-1} in serum or plasma.[53–55] In comparison, ELISA protocols usually reach a LOD of about 1 μg mL^{-1}.[56] Using the more sophisticated surface plasmon resonance spectroscopy (SPRS), a LOD of 1 μg mL^{-1} for CRP in matrix-free buffer was shown by Meyer *et al.*[57] Using aptamer-coated magnetic beads in combination with a luminometer a LOD of 0.0125 μg mL^{-1} in matrix containing samples was demonstrated.[58] Bini *et al.* were able to reach a LOD of 0.005 μg mL^{-1} in human serum albumin (HSA) spiked buffer solutions with an aptamer based biosensor in combination with SPRS.[18] But this sensor showed clear matrix effects when exposed to 1 : 100 diluted and filtered serum samples. Even diluted serum represents a far more complex mixture of biomolecules than an albumin spiked buffer solution, *e.g.*, the competitive immunoassay of Murphy *et al.* has exhibited a LOD of 0.3 μg mL^{-1} CRP in buffer and 5 μg mL^{-1} in serum.[59]

In our work, sensor assembling and antibody–antigen reactions were traced in real time by using SPRS or SPFS, respectively. In order to reduce possible non-specific interactions between the sensor surface and the test sample, a simple

commonly referenced saturation step with BSA was performed before the analyte contacts.[59,60]

Other authors made use of a directed immobilization of the antibodies leading to antigen-binding sites (variable domain Fab) facing into the solution.[31,57,61] In contrast, we present a simplified sensor architecture being highly sufficient to measure CRP in serum, even with the capturing antibodies randomly orientated at the surface. According to a flexible capture and detection system which can be easily changed, our sensor is expected to be applicable in a wide variety of fields.

2 Materials and methods

2.1 Chemicals and materials

Polydimethylsiloxane (PDMS, Sylgard 184 silicone elastomer kit) was obtained from DOW Corning, USA. Chrome (99.8%) was purchased from Chromtec, Germany and silver (99.99% purity) from Umicore, Germany. 11-Mercaptoundecanoic acid (11-MUA, 95%), 6-mercaptohexanol (6-MHex, 97%), BSA (98%), ethanol (analytical grade), and phosphate buffered saline (PBS, pH 7.4) were purchased from Sigma-Aldrich. *N*-Hydroxysuccinimide (NHS) and 1-ethyl-3-(3-dimethylaminopropyl)-carbodiimide (EDC) were obtained as an amine coupling kit (BR-1000-50) from Biacore. The 10 mM glycine–HCl regeneration buffer (pH 2.5) was purchased from Biacore. For fluorescence labelling of the detection antibodies, the DyLight 649 antibody labelling kit (excitation peak at 646 nm, emission peak at 674 nm) from Thermo Fisher Scientific was used. Ultrapure water was produced with a TKA GenPure UV-TOC/UF water purification system (Thermo Fisher Scientific). Human CRP (AG723) was purchased from Millipore. The monoclonal capture antibody C6 (4C28-C6) and the monoclonal detection antibody C2 (4C28-C2), as well as the CRP free serum (4C27) (CRP, CRP free serum and the antibodies manufactured by HyTest Ltd, Finland), were bought from Biotrend, Germany.

2.2 Flow cell

A home build 70 μL flow cell, similar to the design of Nicol,[62] was used for all measurements. A detailed description of the flow cell assembly is given in the ESI.† The solvent flow was generated by a peristaltic pump (Ismatec Reglo, Switzerland), connected to the flow cell by Tygon tubing 2001 (ID 0.38 mm, Ismatec). The circulating total sample volume was 1000 μL (including the volume of all tubing and of the flow cell) with a flow rate of 10 μL min^{-1}.

2.3 Sensor preparation

A 2 nm thick chrome layer (used as an adhesion layer for silver) and a 45 nm thick silver film were evaporated with a thermal evaporator (Auto 306, BOC Edwards) onto LaSFN9 glass slides ($n = 1.846$ at $\lambda = 632.8$ nm, Hellma, Germany) at evaporation rates of 0.5 nm s^{-1} for Cr and 1 nm s^{-1} for Ag at a process pressure of $\sim 7 \times 10^{-6}$ hPa. Following evaporation the prepared metal films were cooled down under high vacuum. Self-assembling of the mixed thiol monolayer (SAM) was then performed immediately by coadsorption out of a 1 : 3 thiol mixture containing 7.5 mM 6-MHex ($HS–C_6H_{12}–OH$) and 2.5 mM 11-MUA ($HS–C_{10}H_{20}–COOH$) in absolute ethanol for 3 h according to Briand *et al.*[63] As shown by Vareiro *et al.*[31] and Schneider *et al.*[64] it is recommended to dilute the SAM laterally. Due to a possible steric hindrance of the capture antibodies 6-MHex was used as a lateral spacer for 11-MUA. The carboxylic groups of the SAM were activated with a mixture of 400 mM NHS and 50 mM EDC in ultrapure water for 2 h.[63] Afterwards, the anti-CRP capture antibody C6 solution (50 μg mL^{-1} PBS, pH 7.4) was circulated over the SAM for about 120 min. The remaining (activated) carboxyl groups were inactivated and the sensor surface was saturated by using a 1.5 mM BSA–PBS solution.[60] Except for the SAM preparation, the entire sensor preparation was performed in the flow cell. Every preparation step was followed by a washing step with PBS (pH 7.4) for 5 min. The sensor architecture is depicted in Fig. S-1 (see ESI†).

2.4 Antibody labelling

The labelling of the detection antibodies was performed using the above mentioned DyLight 649 antibody labelling kit following the manufacturer's instructions and is described briefly under the ESI.†

2.5 Instrumentation

Measurements were performed on a SPFS spectrometer (RT2005, Resonant Technologies GmbH, Germany) in Kretschmann configuration.[65] The instrumentation is based on a design by Yu *et al.*[34] A more detailed description of the used set-up as well of the theoretical background is given in the ESI.†

2.6 Measurements

In situ assembling of the sensor surface was monitored in the kinetic mode at a fixed angle of incidence, adjusted to a reflectivity of 30% within the linear part of the surface plasmon resonance. Antibody and CRP-binding kinetics were followed by recording the shift of the resonance angle, where the excitation of the fluorophore is at its maximum. For calculating the optical thickness, SPRS-scan measurements were taken before and after the desired adsorption and assembling steps, respectively, and analyzed as described in the ESI.†

In order to examine possible interactions between the sensor surface and reagents, pre-tests were performed. First, the interaction between CRP and the SAM was analyzed. Therefore, a SAM was prepared as described above. Without the NHS/EDC activation step, a 50 μg mL^{-1} of CRP–PBS solution was circulated for 15 min over the SAM. Finally, a washing step with PBS was performed for 5 min and a final scan measurement was taken. Second, the SAM was directly saturated by circulating a 1.5 mM BSA–PBS solution for 15 min over the SAM at identical conditions, subsequently followed by a PBS washing step. Afterwards, 100 μg mL^{-1} CRP in PBS was added and circulated for 5 min, also followed by a washing step and a scan measurement. Furthermore, the sensor's background noise was tested with CRP free serum in order to observe if any relevant non-specific interactions occurred. Testing was performed as described below, without addition of the CRP to the serum.

In order to determine the sensor's LOD, measurements were performed in CRP spiked buffer and serum. A stock solution of 1 μg mL^{-1} CRP in PBS (pH 7.4) was freshly prepared prior to the experiments. This solution was further diluted with PBS to the desired final CRP concentrations of 0.001, 0.01, 0.1 and 1.0 μg mL^{-1}. For measurements in matrix the same CRP concentrations were used with PBS 1 : 20 diluted serum.[66] In addition, a concentration range from 0.001 μg mL^{-1} up to 25 μg mL^{-1} was measured as well.

The CRP containing samples were added to the sensor and circulated in the flow cell for 5 min, followed by a 5 min washing step with PBS (pH 7.4) to remove unbound CRP and matrix compounds. Immediately afterwards, the detection antibody solution (50 μg mL^{-1} PBS, pH 7.4) was injected into the flow cell and circulated for 5 min. Again, a further PBS washing step was carried out for 5 min. After each measured concentration, the sensor was regenerated by applying regeneration buffer for 2 min. The antibody–antigen reactions were monitored by kinetic measurements of the fluorescence signal and of the resonance angle shift. Scan measurements before and after adsorption steps have been performed for optical thickness calculations. This has been done also in combination with fluorescence detection to calculate the maximal fluorescence signal resulting from CRP-binding. All measurements have been performed at room temperature.

For the calculation of the optical thicknesses (d) the following dielectric constants ($\varepsilon'/\varepsilon''$) were used: chrome: −4/18, silver: −15.9/1.03, SAM: 2.16/0,[67] mAB, BSA and CRP: 2.1025/0,[68] PBS: 1.773/0. Except for the metal films, it is assumed that the dielectric constant consists only of a real part. The imaginary part was kept zero.

2.7 Data analysis

The mean values of the fluorescence signals resulting from binding of the detection antibody, corrected by the background noise, were plotted against the used CRP concentrations. The resulting concentration–response curves in serum and buffer were then fitted applying the Hill equation.

The LOD was calculated using the equation from Naushad *et al.* by applying 3.3-times of the standard deviation (SD) of the blank response (background noise) of the recovered sensor after CRP addition[69] (see S-eqn (1), ESI†). The LOQ was calculated by considering tenfold of the SD.

In order to get information about the sensitivity of the sensor, the mass coverage of the sensor, especially of CRP-binding onto the capture antibody, was calculated using Fejter's formula (see S-eqn (2), ESI†) as described by Duque *et al.*[70]

More information on data analysis is given in the ESI.†

3 Results and discussion

3.1 Pre-tests

The SAM thickness of ~1.5 nm was experimentally determined by SPRS-scan measurements (data not shown). After adding 50 μg mL^{-1} CRP solution to the SAM, surface interactions between CRP and the non-activated SAM could be observed. As visualized in Fig. S-2 (see ESI†), an angle shift towards a larger resonance angle of 0.225 ± 0.025° occurred, which corresponds to an increase in optical thickness of about 1.25 ± 0.07 nm (m = 2). This leads to a calculated mass coverage of 0.82 ± 0.05 ng mm^{-2}, which equates to a coverage of 11% in comparison to an ideal CRP layer with an calculated mass coverage of 7.25 ng mm^{-2} by assumption of a theoretical optical thickness of 11 nm for CRP.[71]

In contrast, CRP interaction with the SAM after surface saturation with BSA was almost not traceable (see Fig. S-3, ESI†). Furthermore, after the inactivation of the surface with BSA, no further adsorption of serum proteins could be detected (Fig. S-4, ESI†). Therefore, and because the bound antibodies were still able to capture CRP as shown below by SPFS measurements of the detection reaction, BSA was used as the inactivation agent.

3.2 Sensor preparation

The kinetics of the *in situ* sensor preparation steps are shown in Fig. S-5 (see ESI†). After the activation step with NHS/EDC of the carboxylic groups of the SAM by formation of an active ester (not shown) the capture antibodies (anti-CRP) were bonded to the SAM. This resulted in an increase in reflectivity. Finally the inactivation/saturation steps with BSA were carried out. In order to calculate the optical thickness of the anti-CRP layer and of the BSA-saturated anti-CRP layer, scan measurements were performed (Fig. 1). The optical thickness calculated from these scans was found to be 4.40 ± 0.6 nm (m = 6) for the anti-CRP (capture antibody) layer and 4.98 ± 0.59 nm (m = 6) for the anti-CRP/BSA layer. Thus, BSA did cause only a slight increase in layer thickness. We therefore conclude that there is no major interaction present between the anti-CRP and BSA, and the BSA very probably occupies the gaps in the imperfect antibody layer enhancing the layer density and with this the overall optical thickness. The calculation of the mass coverage results in 2.90 ± 0.39 ng mm^{-2} for the capture antibody layer and 3.28 ± 0.36 ng mm^{-2} for the antibody/BSA layer. With respect to the

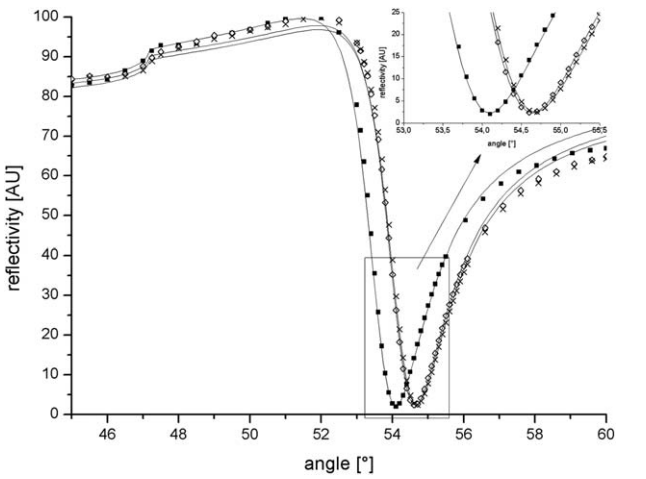

Fig. 1 SPRS-scans including fits (-) of the SAM (■) after activation, after binding of the capture antibody (◇) and after addition of BSA (X). The inset shows a magnification of the particular resonance angles.

optical thickness which can be theoretically achieved by a densely packed capture antibody layer (~16 nm for IgG[72]), the mass coverage was calculated to be ~27.5% for the antibody layer and ~31% for the antibody/BSA layer.

Schneider *et al.* used avidin/biotin anchored antibodies against hCG on a SiO_2 surface saturated with polyethylene glycol (PEG).[64] The hCG sensor reached a hCG-antibody mass coverage of 3.52 ng mm^{-2}. The antibody mass coverage of our biosensor is only slightly below the mass coverage achieved by Schneider *et al.*[64]

3.3 CRP measurements

By exposing the sensor to CRP free 1 : 20 diluted serum, an angle shift could be observed with SPRS. Nevertheless, after washing with PBS, the angle shift decreased, indicating a substantial recovery of the surface. This can be explained by a minor non-specific adhesion of serum proteins onto the sensor surface, which implies that inactivation by BSA cannot completely prevent non-specific binding of matrix components. However, no non-specific interference between detection antibody and the sensor could be detected with SPFS (see S-6, ESI†). Tarkkinen *et al.* utilised the same detection antibody for CRP in their work, however the antibodies were not labeled in the same way, and the immunoassay was based on antibody decorated microparticles.[73] The reported test results obtained in highly diluted patient blood samples ($m = 100$) correlated well with results obtained with the Dade Behring N High-Sensitivity CRP assay. From the reported results we conclude that Tarkkinen *et al.* did not observe relevant non-specific interferences, otherwise they would not have observed good correlation between both methods. As assay specificity is largely defined by the specificity of the antibody (particularly of the detection antibody in this instance), we did not perform specific experiments to resolve "specific non-specificity" with respect to the cross-reactivity of our sensor (*e.g.* due to possible degraded forms and post-translational modifications of CRP or other pathologically relevant proteins). Our assay made use of two monoclonal antibodies targeting distinct CRP-epitopes. It is very unlikely that other serum components would present two similar epitopes, thus cross-reactivities are less likely. However, several factors (*e.g.* pH, surface charges, antibody labeling) can negatively influence the specificity of immunoassays, such as causing conformational changes of the antigen-binding site. Therefore, to fully elucidate possible interferences, further specific experiments addressing this issue, in addition to testing the influence of pathologically elevated blood components such as rheumatoid factors (antibody against Fc-subunit of IgG) and additives used in blood sampling devices, would be needed. The latter will be part of the future work, along with further investigation into the applicability of the sensor in other biological matrices.

Špringer *et al.* did show on their BSA-saturated hCG sensor (anchored via streptavidin/biotin) a more sufficient reduction of non-specific adsorption of serum components, when the sensor was rinsed with a special buffer,[74] than found with our sensor system.

Sensors based on zwitterionic polymers with antifouling properties had shown a mass coverage by matrix components nearly undetectable with a SPR detection scheme.[75,76] In contrast to those sensors, our sensor design did not make use of materials with real antifouling properties. Therefore, a higher adsorption of matrix components can be expected. But it has to be pointed out as a major advantage that our design is far less complex in sensor architecture and much faster in sensor preparation.

By calculating the mass coverage after adding CRP in buffer, the efficiency of the capture layer can be estimated. With maximal saturation at 25 μg mL^{-1} of CRP in PBS, the determined layer thickness of the antibody-bound CRP was 0.43 + 0.06 nm. This leads to a mass coverage of 0.28 + 0.04 ng mm^{-2}. Hence, only ~9.7% of the capture antibody epitopes were accessible by CRP, which is not surprising, as a randomly orientated capture antibody sensor architecture was used. Furthermore, the determined mass coverage is in good agreement with Schneider *et al.*[64] With randomly orientated surface bound antibodies on a PEG saturated sensor Schneider *et al.* achieved a mass coverage of 0.26 ng mm^{-2} for the captured hCG.

Only at CRP concentrations ≥1 μg mL^{-1} an increasing detection antibody layer thickness could be recognized with SPRS in buffer (Fig. 2). Thus only at these CRP concentrations SPRS did show sufficient sensitivity. These findings are in agreement with the results from Meyer *et al.* who had reported a CRP detection limit of 2 μg mL^{-1} with SPRS.[57] In comparison to the SPRS signal the corresponding SPFS signal shown in Fig. 2 is much larger, emphasizing the potential of SPFS. As depicted in Fig. 2, equilibrium of the capture antibody-CRP, respectively of the CRP detection antibody reaction, is reached within minutes. With further optimization of the incubation time,

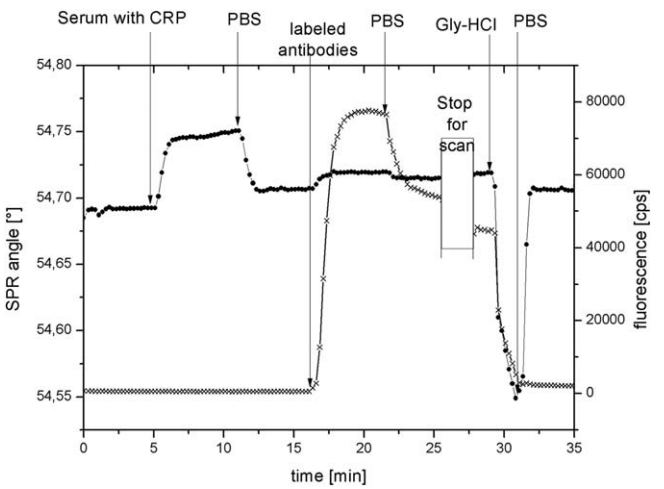

Fig. 2 Simultaneous measured SPRS (●)- and SPFS (X)-kinetics of the time dependent response of the CRP-sensor in serum. The plot shows a section of the whole dose–response curve at 1 μg mL^{-1} CRP. First the CRP containing serum sample was added and circulated for 5 min. A rinsing step was applied afterwards, followed by the addition of the fluorescence labeled detection antibody. To remove unbound detection antibodies the sensor was rinsed again before the sensor was regenerated for measuring the next concentration.

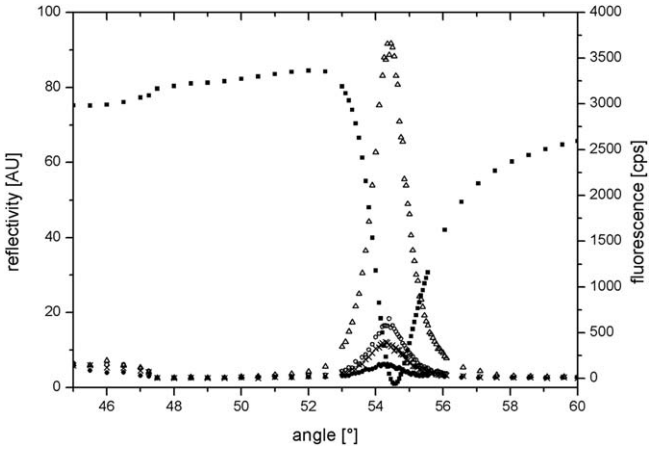

Fig. 3 Fluorescence intensity investigation at the surface plasmon resonance for 0 μg mL^{-1} (●), 0.001 μg mL^{-1} (x), 0.01 μg mL^{-1} (◇) and 0.1 μg mL^{-1} CRP (Δ) in serum. Also shown is the SPRS-scan taken at a CRP concentration of 0.1 μg mL^{-1}. As noticeable, the peak maximum of the fluorescence signal is located at a slightly lower angle of incidence than the reflectivity minimum of the corresponding SPR-curve.[38]

measurements could be carried out in a fraction of the time. Furthermore, Fig. 2 shows that the applied sensor regeneration procedure was sufficient as visualized by the decline of the fluorescence signal during the rinsing step with glycine–HCl-recovery buffer. Recovery of the sensor was possible over at least 8 repeated cycles, enduring measurements over the whole concentration range of the reported CRP concentration–response curve (Fig. 4). However, with SPFS CRP was already traceable at a concentration of 0.001 μg mL^{-1} (see Fig. 3). The corresponding fluorescence signal did already differ remarkably from the background signal and did increase significantly with increasing CRP concentrations. Fig. S-7 (see ESI†) shows the resulting SPFS signals at higher CRP concentrations. At concentrations >1 μg mL^{-1} saturation of the sensor occurs.

3.4 LOD and LOQ

For the determination of the LOD and LOQ different CRP concentrations were applied to the sensor either in 1 : 20 diluted serum or in PBS. The fluorescence intensity increased with respect to increasing CRP concentrations. As shown in Fig. 4, the major increase of the fluorescence signal occurred between 0.01 μg mL^{-1} CRP and 1 μg mL^{-1} CRP. The resulting fluorescence signal at different CRP concentrations was plotted against the CRP concentration measured in PBS (number of measurements (m) = 2, therefore the error is given as maximum error) and in 1 : 20 diluted serum (m = 3) (Fig. 4). For calculating the LOD, Naushad's formula (see S-eqn (1), ESI†) was applied. Therefore, the slopes (S) were calculated by applying the linear equation at CRP concentrations between 0.01 μg mL^{-1} and 1 μg mL^{-1} in buffer and 1 : 20 diluted serum, respectively.

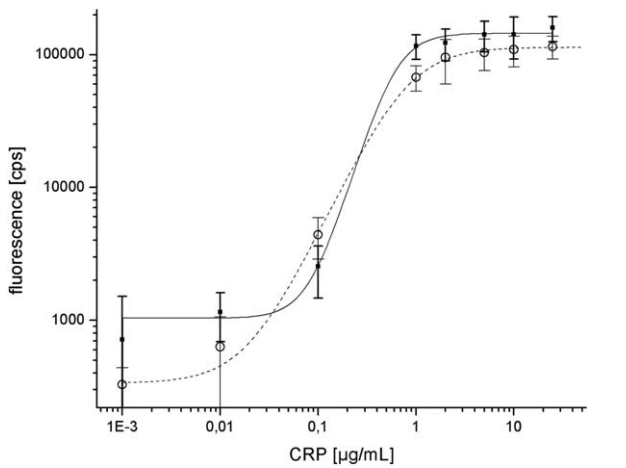

Fig. 4 CRP concentration–response curve measured in PBS (■) and serum (○).

Both CRP concentration–response curves did show good linear correlation (R^2 = 0.999 for serum and 0.994 for buffer) at this concentration range. The calculated S in buffer of 118 927 and in serum of 68 094 was used. The calculated standard deviation (SD) of the background signals (m = 8) for the PBS was ±582 cps. This leads to a LOD for CRP in buffer of 0.016 μg mL^{-1}. For CRP in serum containing assays, a LOD of 0.026 μg mL^{-1} was calculated with a SD (m = 12) of ±541 cps. Similar to the calculation of the LOD, LOQ was calculated but by applying the tenfold of the SD resulting in an LOQ in buffer of 0.049 μg mL^{-1} and 0.08 μg mL^{-1} in 1 : 20 diluted serum. The calculated LOD in serum from SPFS measurements is much lower than the LOD of 2 μg mL^{-1} found with SPRS by Meyer *et al.*[57] for CRP in BSA spiked buffer. The LOD of 0.01 μg mL^{-1} for hCG in serum found by Špringer *et al.* with SPRS was 2.6 times lower than that determined with our sensor measured with SPFS.[74] To our knowledge, only a few papers in the literature have reported about the determination of the LOD in serum using SPFS. Wang *et al.* had published a SPFS biosensor for detecting prostate specific antigen (PSA) in buffer and serum.[77] For this purpose, they had bound antibodies in a carboxymethyl dextran hydrogel after its swelling in buffer. The detection of PSA was performed with fluorescent labeled antibodies too. With this sensor design, they had reached a LOD of 330 fM in serum. Our LOD in serum amounted to 0.026 μg mL^{-1}. Considering the molecular weight of the pentraxin CRP (105 kDa), the LOD is 248 pM. The SPFS-detection of PSA in serum with a similar antibody-decorated carboxymethyl dextran sensor with an LOD of ~2 pg mL^{-1} (~80 fM) was reported by Yu *et al.*[32] In contrast to our sensor design, the sensors of Wang *et al.* and Yu *et al.* made use of the antifouling property of carboxymethyl dextran hydrogel.[32,77] Thus the lower LOD is of no surprise. Li *et al.* had shown a LOD for CRP with a new microfluidic fluorescence heterogeneous immunoassay of 0.36 μg mL^{-1},[78] which is also higher than the presented LOD. Furthermore, the obtained LOD and LOQ of our sensor are in the range provided by commercial CRP detection platforms widely used in routine analysis.

4 Conclusions

Compared with other test devices, the SPFS in combination with the presented biosensor had shown a low LOD of 0.016 μg mL^{-1} in buffer and 0.026 μg mL^{-1} in serum for CRP. The LOQ in buffer was 0.049 μg mL^{-1} and 0.08 μg mL^{-1} in 1 : 20 diluted

serum. The sensor did show a sufficient LOD and LOQ in serum to detect pathologically relevant CRP concentrations. Moreover, even the assessment of CVD risk should be possible with this sensor. So far, only a few test devices used the same detection methods (SPFS, SPRS) and comparable, but more complex, sensor architectures in comparison to the presented work. However, most of those sensors did show a LOD in the same range than our sensor. A few sensors achieved an even lower LOD. In contrast to our sensor, most published sensor designs are comparably very complex, which is a real drawback from an economical point of view. More chemicals have to be used for the fabrication and the fabrication itself becomes more difficult as more steps are needed. Our presented sensor shows a good economical and ecological compromise with respect to the LOD and LOQ, not least because of its reusability. Using current protocols a single CRP measurement takes approximately 20 min. As observed in the kinetic measurements, equilibration of the antibody–antigen reaction is rapid and can be observed in real time, thus the total experimental time could be considerably shortened, giving rise to the possibility of rapid measurements. Extended incubation times, as required for ELISAs and FLISAs, would be thus not required. CRP can, to some extent, be used as a diagnostic indicator for acute inflammatory events, such as evolvement of life-threatening systemic infections[79] and can be utilized for therapy control. In such cases, rapid determination of CRP is favoured in order to provide the patient with the best medical treatment and outcome. Procalcitonin has recently been proposed as an essential biomarker to differentiate between bacterial and non-bacterial inflammatory events.[80] The simultaneous determinations of CRP and procalcitonin, or of other analytes, would be of advantage in terms of analysis and diagnosis speed, cost effectiveness, and sample and material consumption. In principle, microarray measurements can be achieved by performing surface plasmon enhanced fluorescence microscopy.[81] Therefore, the proof of applicability of our sensor design in other complex biological matrices such as urine, saliva and faeces, as well as to other marker proteins, will be part of future work.

Acknowledgements

The authors thank Prof. P. M. Schneider, Institute of Legal Medicine, Medical Faculty, University of Cologne, Germany, and Prof. S. Mittler, Dept. of Physics and Astronomy, University of Western Ontario, Canada, for fruitful discussions, Dr J. D. Mercer-Chalmers, University of Bath, UK, for proofreading, G. Herrmann and N. Horn, Max Planck-Institute for Polymer Research, Mainz, Germany, for their technical support in preparing metal films.

References

1 M. Thevis, I. Maurer, M. Kohler, H. Geyer and W. Schanzer, *Int. J. Sports Med.*, 2007, **28**, 545–549.
2 S. J. Larson, J. M. Holler, J. Magluilo, C. S. Dunkley and A. Jacobs, *J. Anal. Toxicol.*, 2008, **32**, 438–443.
3 A. Dasgupta, *Am. J. Clin. Pathol.*, 2007, **128**, 491–503.
4 A. Dasgupta, *Med. Lab. Obs.*, 2008, **40**, 24–25.
5 W. B. Jaffee, E. Trucco, S. Levy and R. D. Weiss, *J. Subst. Abuse Treat.*, 2007, **33**, 33–42.
6 S. Iwersen-Bergmann, P. Rieger, S. W. Toennes, R. Keller and G. F. Kauert, *presented in part at the XVI. GTFCh-Symposium: Toxikologie psychisch aktiver Substanzen*, Mosbach, Germany, 2009.
7 A. Scholer, *Toxichem. Krimtech.*, 2004, **71**, 127–137.
8 A. Thomas, M. Kohler, K. Walpurgis, W. Schanzer and M. Thevis, *Drug Test. Anal.*, 2009, **1**, 81–86.
9 J. L. Brash and T. A. Horbett, in *Proteins At Interfaces II*, American Chemical Society, 1995, vol. 602, pp. 1–23.
10 T. A. Horbett and J. L. Brash, *ACS Symp. Ser.*, 1987, **343**, 1–33.
11 E. D. Kaufman, J. Belyea, M. C. Johnson, Z. M. Nicholson, J. L. Ricks, P. K. Shah, M. Bayless, T. Pettersson, Z. Feldoto, E. Blomberg, P. Claesson and S. Franzen, *Langmuir*, 2007, **23**, 6053–6062.
12 C. Czeslik, *Chem. Unserer Zeit*, 2006, **40**, 238–245.
13 B. Liedberg, C. Nylander and I. Lunström, *Sens. Actuators*, 1983, **4**, 299–304.
14 S. Lofas, M. Malmqvist, I. Ronnberg, E. Stenberg, B. Liedberg and I. Lundstrom, *Sens. Actuators, B*, 1991, **5**, 79–84.
15 W. Knoll, *Annu. Rev. Phys. Chem.*, 1998, **49**, 569–638.
16 W. M. Mullett, E. P. C. Lai and J. M. Yeung, *Methods*, 2000, **22**, 77–91.
17 R. L. Rich and D. G. Myszka, *J. Mol. Recognit.*, 2006, **19**, 478–534.
18 A. Bini, S. Centi, S. Tombelli, M. Minunni and M. Mascini, *Anal. Bioanal. Chem.*, 2008, **390**, 1077–1086.
19 S. D. Carrigan and M. Tabrizian, *Langmuir*, 2005, **21**, 12320–12326.
20 P. Kingshott and H. J. Griesser, *Curr. Opin. Solid State Mater. Sci.*, 1999, **4**, 403–412.
21 L. Li, S. Chen, J. Zheng, B. D. Ratner and S. Jiang, *J. Phys. Chem. B*, 2005, **109**, 2934–2941.
22 S. Löfas and B. Johnsson, *J. Chem. Soc., Chem. Commun.*, 1990, 1526–1528.
23 R. E. Marchant, S. Yuan and G. Szakalas-Gratzl, *J. Biomater. Sci., Polym. Ed.*, 1995, **6**, 549–564.
24 E. Österberg, K. Bergström, K. Holmberg, J. A. Riggs, J. M. Van Alstine, T. P. Schuman, N. L. Burns and J. M. Harris, *Colloids Surf., A*, 1993, **77**, 159–169.
25 M. Adamczyk, J. A. Moore and Z. Yu, *Methods*, 2000, **20**, 319–328.
26 J. E. Gestwicki, H. V. Hsieh and J. B. Pitner, *Anal. Chem.*, 2001, **73**, 5732–5737.
27 R. Karlsson, *Anal. Biochem.*, 1994, **221**, 142–151.
28 T. Liebermann, W. Knoll, P. Sluka and R. Herrmann, *Colloids Surf., A*, 2000, **169**, 337–350.
29 J. Malicka, I. Gryczynski, Z. Gryczynski and J. R. Lakowicz, *J. Phys. Chem. B*, 2004, **108**, 19114–19118.
30 E. Matveeva, Z. Gryczynski, I. Gryczynski, J. Malicka and J. R. Lakowicz, *Anal. Chem.*, 2004, **76**, 6287–6292.
31 M. M. Vareiro, J. Liu, W. Knoll, K. Zak, D. Williams and A. T. Jenkins, *Anal. Chem.*, 2005, **77**, 2426–2431.
32 F. Yu, B. Persson, S. Lofas and W. Knoll, *Anal. Chem.*, 2004, **76**, 6765–6770.

33 F. Yu, B. Persson, S. Löfas and W. Knoll, *J. Am. Chem. Soc.*, 2004, **126**, 8902–8903.
34 F. Yu, D. Yao and W. Knoll, *Anal. Chem.*, 2003, **75**, 2610–2607.
35 J. S. Yuk, G. N. Gibson, J. M. Rice, E. F. Guignon and M. A. Lynes, *Analyst*, 2012, **137**, 2574–2581.
36 J. S. Yuk, C. McDonagh and B. D. MacCraith, *Anal. Bioanal. Chem.*, 2010, **398**, 1947–1954.
37 T. Liebermann and W. Knoll, *Colloids Surf., A*, 2000, **171**, 115–130.
38 T. Liebermann and W. Knoll, *Langmuir*, 2003, **19**, 1567–1572.
39 B. Liedberg, C. Nylander and I. Lundstrom, *Sens. Actuators*, 1983, **4**, 299–304.
40 S. Kienle, S. Lingler, W. Kraas, A. Offenhäusser, W. Knoll and G. Jung, *Biosens. Bioelectron.*, 1997, **12**, 779–786.
41 G. Stengel and W. Knoll, *Nucleic Acids Res.*, 2005, **33**, e69.
42 J. Masson, T. Battaglia, J. Cramer, S. Beaudoin, M. Sierks and K. Booksh, *Anal. Bioanal. Chem.*, 2006, **386**, 1951–1959.
43 M. Farre, E. Martinez, J. Ramon, A. Navarro, J. Radjenovic, E. Mauriz, L. Lechuga, M. Marco and D. Barcelo, *Anal. Bioanal. Chem.*, 2007, **388**, 207–214.
44 M. P. de Maat and C. Kluft, *Ital. Heart J.*, 2001, **2**, 189–195.
45 S. Black, I. Kushner and D. Samols, *J. Biol. Chem.*, 2004, **279**, 48487–48490.
46 J. Li and C. Fang, *Med. Hypotheses*, 2004, **62**, 499–506.
47 S. P. Mazer and L. E. Rabbani, *J. Thromb. Thrombolysis*, 2004, **17**, 95–105.
48 T. A. Pearson, G. A. Mensah, R. W. Alexander, J. L. Anderson, R. O. Cannon, M. Criqui, Y. Y. Fadl, S. P. Fortmann, Y. Hong, G. L. Myers, N. Rifai, S. C. Smith, K. Taubert, R. P. Tracy and F. Vinicor, *Circulation*, 2003, **107**, 499–511.
49 J. L. Clarke, J. L. Anderson, J. F. Carlquist, R. F. Roberts, B. D. Horne, T. L. Bair, M. J. Kolek, C. P. Mower, A. M. Crane, W. L. Roberts and J. B. Muhlestein, *Am. J. Cardiol.*, 2005, **95**, 155–158.
50 O. Deegan, K. Walshe, K. Kavanagh and S. Doyle, *Anal. Biochem.*, 2003, **312**, 175–181.
51 R. Dominici, P. Luraschi and C. Franzini, *J. Clin. Lab. Anal.*, 2004, **18**, 280–284.
52 M. D. Parra, M. Tuomola, J. Cabezas-Herrera and J. J. Ceron, *Am. J. Vet. Res.*, 2005, **66**, 62–66.
53 T. Q. Wei, S. Kramer, V. P. Chu, D. Hudson, D. Kilgore, S. Salyer, G. Parker, A. Eyberger, R. Arentzen and H. Koiv, *J. Autom. Methods Manage. Chem.*, 2000, **22**, 125–131.
54 Roche Diagnostics GmbH, *Tina-quant Cardiac C-reactive Protein (Latex) High Sensitivie (Product Specification Sheet)*, 2009.
55 Roche Diagnostics GmbH, *Tina-quant C-reactive Protein Gen. 3 (Product Specification Sheet)*, 2009.
56 T. B. Ledue and N. Rifai, *Clin. Chem. Lab. Med.*, 2001, **39**, 1171–1176.
57 M. H. F. Meyer, M. Hartmann and M. Keusgen, *Biosens. Bioelectron.*, 2006, **21**, 1987–1990.
58 Y.-N. Yang, H.-I. Lin, J.-H. Wang, S.-C. Shiesh and G.-B. Lee, *Biosens. Bioelectron.*, 2009, **24**, 3091–3096.
59 B. M. Murphy, X. He, D. Dandy and C. S. Henry, *Anal. Chem.*, 2008, **80**, 444–450.
60 H. Aizawa, M. Tozuka, S. Kurosawa, K. Kobayashi, S. M. Reddy and M. Higuchi, *Anal. Chim. Acta*, 2007, **591**, 191–194.
61 H. Y. Lin, W. P. Hu, H. Y. Hsu, A. Chiou, G. L. Chang, K. Y. Tseng and S. J. Chen, *Biosens. Bioelectron.*, 2006, **21**, 1631–1637.
62 A. Nicol, PhD thesis, Johannes Gutenberg-Universität Mainz, 2005.
63 E. Briand, M. Salmain, J. Herry, H. Perrot, C. Compere and C. Pradier, *Biosens. Bioelectron.*, 2006, **22**, 440–448.
64 B. H. Schneider, E. L. Dickinson, M. D. Vach, J. V. Hoijer and L. V. Howard, *Biosens. Bioelectron.*, 2000, **15**, 13–22.
65 E. Kretschmann, *Z. Phys. A: Hadrons Nucl.*, 1971, **241**, 313–324.
66 T. Nagel, N. Gajovic-Eichelmann, S. Tobisch, U. Schulte-Spechtel and F. F. Bier, *Clin. Chim. Acta*, 2008, **394**, 110–113.
67 C. M. Pettit and D. Roy, *Analyst*, 2007, **132**, 524–535.
68 T. Neumann, PhD thesis, Johannes Gutenberg-Universität Mainz, 2001.
69 M. Naushad, M. Aqil, F. Ahmad, A. Ali, M. Faisal, M. Rizwan and S. Faiyaz, *J. Anal. Chem.*, 2008, **63**, 965–970.
70 L. Duque, B. Menges, S. Borros and R. Förch, *Biomacromolecules*, 2010, **11**, 2818–2823.
71 S. Lin, C.-K. Lee, Y.-M. Wang, L.-S. Huang, Y.-H. Lin, S.-Y. Lee, B.-C. Sheu and S.-M. Hsu, *Biosens. Bioelectron.*, 2006, **22**, 323–327.
72 B. Hanley, L. Xing and R. H. Cheng, *Theor. Biol. Med. Modell.*, 2007, **4**, 31.
73 P. Tarkkinen, T. Palenius and T. Lövgren, *Clin. Chem.*, 2002, **48**, 269–277.
74 T. Špringer, M. Piliarik and J. Homola, *Anal. Bioanal. Chem.*, 2010, 1–7.
75 C. Rodriguez-Emmenegger, E. Brynda, T. Riedel, Z. Sedlakova, M. Houska and A. B. Alles, *Langmuir*, 2009, **25**, 6328–6333.
76 H. Vaisocherová, W. Yang, Z. Zhang, Z. Cao, G. Cheng, M. Piliarik, J. Homola and S. Jiang, *Anal. Chem.*, 2008, **80**, 7894–7901.
77 Y. Wang, A. Brunsen, U. Jonas, J. Dostalek and W. Knoll, *Anal. Chem.*, 2009, **81**, 9625–9632.
78 P. Li, A. Sherry, J. Cortes, C. Anagnostopoulos and M. Faghri, *Biomed. Microdevices*, 2011, 1–9.
79 R. Sierra, J. Rello, M. A. Bailén, E. Benitez, G. Antonio, L. Cristobal and P. Sebastian, *Intensive Care Med.*, 2004, **30**, 2038–2045.
80 N. Aikawa, S. Fujishima, S. Endo, I. Sekine, K. Kogawa, Y. Yamamoto, S. Kushimoto, H. Yukioka, N. Kato, K. Totsuka, K. Kikuchi, T. Ikeda, K. Ikeda, K. Harada and S. Satomura, *J. Infect. Chemother.*, 2005, **11**, 152–159.
81 R. Robelek, L. F. Niu, E. L. Schmid and W. Knoll, *Anal. Chem.*, 2004, **76**, 6160–6165.

